



## NRC Publications Archive Archives des publications du CNRC

### **Effect of manganese and silicon on iron intermetallics in 206 foundry alloy**

Liu, Kun; Cao, Xinjin; Chen, X. -Grant

This publication could be one of several versions: author's original, accepted manuscript or the publisher's version. /  
La version de cette publication peut être l'une des suivantes : la version prépublication de l'auteur, la version acceptée du manuscrit ou la version de l'éditeur.

#### **Publisher's version / Version de l'éditeur:**

*Light Metals, Advances in Materials and Processes: Proceedings of the 49th Conference of Metallurgists COM 2010, October 3-6, 2010, Vancouver, BC, Canada, pp. 113-120, 2010*

#### **NRC Publications Record / Notice d'Archives des publications de CNRC:**

<https://nrc-publications.canada.ca/eng/view/object/?id=5f06bc30-0c20-46cd-8284-d444b8f60195>

<https://publications-cnrc.canada.ca/fra/voir/objet/?id=5f06bc30-0c20-46cd-8284-d444b8f60195>

Access and use of this website and the material on it are subject to the Terms and Conditions set forth at

<https://nrc-publications.canada.ca/eng/copyright>

READ THESE TERMS AND CONDITIONS CAREFULLY BEFORE USING THIS WEBSITE.

L'accès à ce site Web et l'utilisation de son contenu sont assujettis aux conditions présentées dans le site

<https://publications-cnrc.canada.ca/fra/droits>

LISEZ CES CONDITIONS ATTENTIVEMENT AVANT D'UTILISER CE SITE WEB.

**Questions?** Contact the NRC Publications Archive team at

PublicationsArchive-ArchivesPublications@nrc-cnrc.gc.ca. If you wish to email the authors directly, please see the first page of the publication for their contact information.

**Vous avez des questions?** Nous pouvons vous aider. Pour communiquer directement avec un auteur, consultez la première page de la revue dans laquelle son article a été publié afin de trouver ses coordonnées. Si vous n'arrivez pas à les repérer, communiquez avec nous à PublicationsArchive-ArchivesPublications@nrc-cnrc.gc.ca.



## EFFECT OF MN AND SI ON IRON-CONTAINING INTERMETALLICS IN CAST 206 ALUMINUM ALLOYS

\*Kun Liu<sup>1</sup>, Xinjin Cao<sup>2</sup>, X.-Grant Chen<sup>1</sup>

<sup>1</sup>*Université du Québec à Chicoutimi  
Chicoutimi, Canada, G7H 2B1*

(\*Corresponding author: kun.liu@uqac.ca)

<sup>2</sup>*NRC Institute for Aerospace Research  
Montreal, Canada, H3T 2B2*

### ABSTRACT

Effect of Mn and Si on the formation of iron-containing intermetallic phases has been investigated in Al-4.5%Cu (206) alloy with 0.3% Fe. The iron-containing intermetallics are identified and characterized by using thermal analysis (TA), differential scanning calorimetry (DSC), optical microscope, scanning electron microscope (SEM) and image analysis techniques. It is found that two types of iron-containing intermetallic phases exist in the final solidified structures: platelet  $\beta$ -Fe ( $Al_7Cu_2Fe/Al_7Cu_2(FeMn)$ ) and Chinese script  $\alpha$ -Fe ( $Al_{15}(FeMn)_3(SiCu)_2$ ). Addition of either Mn or Si favors the transformation of  $\beta$ -Fe phase into  $\alpha$ -Fe phase but Mn is more effective than Si. At a combined addition of both Mn and Si to a certain amount, almost all platelet  $\beta$ -Fe can be converted into Chinese script  $\alpha$ -Fe. For a cast of Al-4.5Cu-0.3Fe alloy, 0.3% Mn and 0.3% Si are required to completely suppress the  $\beta$ -Fe phase.



**Light Metals - Advances in Materials and Processes**  
Proceedings of the  
49<sup>th</sup> Annual Conference of Metallurgists of CIM  
Vancouver, BC, Canada  
**Edited by D. Gallienne, M. Bilodeau**

## INTRODUCTION

Iron is one of the most important impurity elements in aluminum alloys. Because of the low solubility of iron in solid aluminum (0.005% at 450°C [1], all alloy compositions in this paper are in wt.%), almost all the iron will precipitate from liquid Al alloys in the form of iron-containing intermetallics which can appear in interdendrites and/or intradendrites in aluminum alloys. To date, several reporters [2-8] have completed abundant work on iron-containing intermetallics in Al-Si cast alloys. Basically, iron-rich phases can be grouped into three kinds of morphologies: polyhedral or star-like, Chinese script and platelet. Hwang *et al.* [6] reported that the polyhedral phase can usually form at a high Mn content as primary iron-containing intermetallics. For the Chinese script phase, generally termed  $\alpha$ -Fe, Cameron *et al.* [7] reported that it is either  $Al_8Fe_2Si$  for low Mn alloys or  $Al_{15}(FeMn)_3Si_2$  for high Mn alloys. The platelet phase is usually thought to be  $\beta$ -Fe ( $Al_3FeSi$ ) [8] and to be detrimental to mechanical properties. In order to decrease the negative effect of  $\beta$ -Fe, one of the most popular ways is to transform the deleterious platelet  $\beta$ -Fe to the less detrimental Chinese script  $\alpha$ -Fe. For this application, neutralization elements are often added to the alloy. Mn is one of the most popularly used neutralization elements. The addition of Mn promotes the formation of the  $\alpha$ -Fe phase and refines the  $\beta$ -Fe phase if it still exists [9]. In Al-12Si-0.4Mg alloy, Cao and Campbell [10] reported a lowest Mn/Fe ratio, approximately 0.17, to start the transformation of the  $\beta$ -Fe phase into the  $\alpha$ -Fe phase. To effectively suppress the formation of the  $\beta$ -Fe phase, Lu *et al.* [2] and Hwang *et al.* [6] suggested an optimal Mn/Fe ratio of around 0.8 in Al-7Si-0.4Mg and 1.2 in Al-7Si-3.8Cu alloys, respectively.

Cast 206 aluminum alloys are widely used in the automotive and aerospace industries because of their high strength and good elevated temperature properties. However, these alloys suffer a great loss of mechanical properties from the presence of small amounts of Fe. In this alloy family, the maximum iron content is usually limited to 0.15% or below (206.0 and 206.2) [11]. In the aerospace applications, the iron content is even restricted below 0.07% (A206.2) [11]. However, with the increasing demand to recycle aluminum alloys, the requirement for low iron contents becomes a big concern from both technique and cost aspects. Therefore, manufacturing premium castings with higher iron contents has become a great challenge. Up to date, however, little work concerning the iron-containing intermetallics and the factors affecting their formation in cast 206 aluminum alloys has been reported. The present study is aimed at investigating the iron-containing intermetallic compounds formed in cast Al-4.5%Cu-0.3%Fe alloys through either individual or combined addition of Mn and Si.

## EXPERIMENTAL

Table 1 shows the chemical compositions of the experimental alloys. Alloy 1 is the base alloy with 0.1Mn and 0.1Si. Alloys 2 and 3, with various Mn contents are designed to investigate the effect of the individual addition of Mn, while Alloys 4 and 5 are used to study the influence of the individual addition of Si. Alloys 6 and 7 are used for the combined effect of both Mn and Si.

The alloys were melted in a resistance furnace at  $\sim 730^\circ\text{C}$ . In each test, approximately 150 g of liquid metal was poured into a preheated, thin-shelled steel crucible. The cooling rate of the thermal analysis samples is about 0.2 K/s. After the full solidification (about  $450^\circ\text{C}$ ), the sample was quenched in the water. The samples were then sectioned, mounted and polished for the metallographic observation. To reveal the three-dimensional morphology of intermetallic phases, some metallographic specimens were deeply etched in a 10% NaOH solution at 60-65°C for 1 to 1.5 minutes. The solidified thermal analysis samples were complementarily tested with a Differential Scanning Calorimeter (DSC) using a Perkin Elmer DSC 7 unit. A JEOL JSM-6480 LV Scanning Electron microscope (SEM) and a Clemex JS-2000 Optical Image Analyzer were used to identify the iron-containing intermetallics and quantify their volume fractions.

Table 1 - Chemical compositions of the alloys used in the experiments

Alloy #	Element (wt. %)								
	Cu	Mg	Fe	Si	Mn	Zn	Ti	Ni	Al
1	4.46	0.27	0.33	<b>0.08</b>	<b>0.11</b>	0.05	0.02	0.02	bal.
2	4.45	0.29	0.31	<b>0.11</b>	<b>0.19</b>	0.05	0.02	0.02	bal.
3	4.52	0.28	0.29	<b>0.11</b>	<b>0.41</b>	0.05	0.02	0.02	bal.
4	4.51	0.29	0.29	<b>0.19</b>	<b>0.09</b>	0.05	0.02	0.02	bal.
5	4.59	0.31	0.31	<b>0.31</b>	<b>0.11</b>	0.05	0.02	0.02	bal.
6	4.48	0.31	0.31	<b>0.21</b>	<b>0.19</b>	0.05	0.02	0.02	bal.
7	4.51	0.32	0.32	<b>0.31</b>	<b>0.31</b>	0.05	0.02	0.02	bal.

**RESULTS AND DISCUSSION**

**Solidification Reactions And Paths**

Fig.1 shows the typical TA and DSC curves in an example of Alloy 6. It can be found that there are five peaks in the TA curve which can also be detected in the DSC heating curve. However, not all the peaks are present in each experimental alloy.

Combing the information obtained from TA, DSC and the observed microstructure, all possible solidification reactions and paths in Alloys 1 to 7 are listed in Table 2. The results agree well in principle to the works of Backerud *et al.* [12] and Lu *et al.* [2]. For a given alloy, the reactions to appear will depend on the alloy compositions. For example, reaction 3 for  $Al_7Cu_2(FeMn)$  is present in Alloy 1 but absent in Alloy 7 while reaction 2 for  $Al_{13}(FeMn)_3(SiCu)_2$  is present in Alloy 7 but disappears in Alloy 1. In other words, the formation of iron-containing intermetallics is clearly related to alloy compositions. After the iron-containing intermetallics formed in these alloys have been identified, the effect of Mn and Si on these iron-containing intermetallics is discussed later.

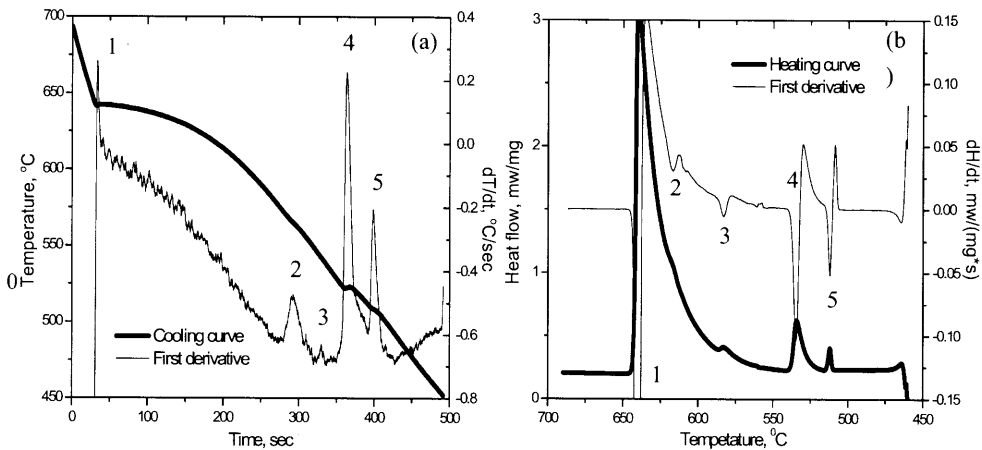


Figure 1 - TA and DSC curves of Alloys 6  
 (a) TA cooling curve and its first derivative, (b) DSC heating curve and its first derivative

Table 2 - Solidification reactions in Alloys 1 to 7

Peak	Reactions	Temp.(°C)*	Alloy
1	A: Aluminum dendrite network forms B: Liq.→Al+Al <sub>6</sub> (MnFeCu)	645~650	1-7
2	Liq.+Al <sub>6</sub> (MnFeCu)→Al+Al <sub>15</sub> (FeMn) <sub>3</sub> (SiCu) <sub>2</sub> .	610~615	2-7
3	Liq.+Al <sub>6</sub> (MnFeCu)→Al+Al <sub>7</sub> Cu <sub>2</sub> (FeMn)	585~595	1-6
4	Liq.→Al+Al <sub>2</sub> Cu+Al <sub>20</sub> Mn <sub>3</sub> Cu <sub>2</sub> +Al <sub>7</sub> Cu <sub>2</sub> Fe	530~540	1-7
5	Liq.→Al+Al <sub>2</sub> Cu+Al <sub>2</sub> CuMg+Mg <sub>2</sub> Si	500~510	4-7

\* Temperature is measured using the DSC heating curve

### Identification of Iron-containing Intermetallic Phases

According to the reactions shown in Table 2, there are several iron-containing intermetallic phases formed in 206 alloys, i.e. Al<sub>6</sub>(MnFeCu), Al<sub>15</sub>(FeMn)<sub>3</sub>(SiCu)<sub>2</sub>, Al<sub>7</sub>Cu<sub>2</sub>(FeMn) and Al<sub>7</sub>Cu<sub>2</sub>Fe. Fig. 2 shows the typical optical microstructures of the various iron-containing intermetallics in the Alloy 3 example. The SEM-EDS (Energy Dispersive X-ray Spectroscopy) results indicate that these iron-containing intermetallics are Al<sub>7</sub>Cu<sub>2</sub>Fe, Al<sub>7</sub>Cu<sub>2</sub>(FeMn) and Al<sub>15</sub>(FeMn)<sub>3</sub>(SiCu)<sub>2</sub>, respectively. The Al<sub>7</sub>Cu<sub>2</sub>(FeMn) phase contains some Mn which replaces some Fe atoms in Al<sub>7</sub>Cu<sub>2</sub>Fe. Therefore, both Al<sub>7</sub>Cu<sub>2</sub>Fe and Al<sub>7</sub>Cu<sub>2</sub>(FeMn) have a platelet morphology and are generally named as being β-Fe phases. In contrast, Al<sub>15</sub>(FeMn)<sub>3</sub>(SiCu)<sub>2</sub> has a Chinese script morphology and is termed as being an α-Fe phase. It should be noticed that another iron-rich phase appearing in reaction 1, Al<sub>6</sub>(MnFeCu), was not observed in the final microstructure, as it was probably completely consumed by reactions 2 and 3. Therefore, the β-Fe phases (Al<sub>7</sub>Cu<sub>2</sub>Fe and Al<sub>7</sub>Cu<sub>2</sub>(FeMn)) and the α-Fe phase (Al<sub>15</sub>(FeMn)<sub>3</sub>(SiCu)<sub>2</sub>) are the main iron-rich phases as generally observed in the final microstructure of Al-4.5Cu alloys.

As shown in Fig. 2a and 2b, the β-Fe phases have a similar platelet shape but different aspect ratios, due to their different formation temperatures. The β-Fe platelet in Fig. 2a is thinner and has higher aspect ratios (15-40) while the β-Fe phase in Fig. 2b is thicker and has smaller aspect ratios (2-11). This indicates that the β-Fe phase in Fig. 2b precipitates at higher temperatures due to the quicker diffusion rate than the β-Fe platelet in Fig. 2a. Their formation corresponds well to reactions 4 and 3 respectively given in Table 2, at 530~540°C for thin Al<sub>7</sub>Cu<sub>2</sub>Fe and 585~595°C for thick Al<sub>7</sub>Cu<sub>2</sub>(FeMn). The thin β-Fe platelet (Al<sub>7</sub>Cu<sub>2</sub>Fe) in Fig. 2a is the product of a eutectic reaction and is thus defined as eutectic β-Fe. However, the thick β-Fe phase (Al<sub>7</sub>Cu<sub>2</sub>(FeMn)) in Fig. 2b precipitates at a higher temperature, prior to the main eutectic reaction (reaction 4), and hence is termed as pre-eutectic β-Fe. The α-Fe phase (Al<sub>15</sub>(FeMn)<sub>3</sub>(SiCu)<sub>2</sub>), has a Chinese script morphology and can only form in alloys with relatively high contents of Mn and/or Si and, as shown in Table 2, its formation temperature is about 610°C.

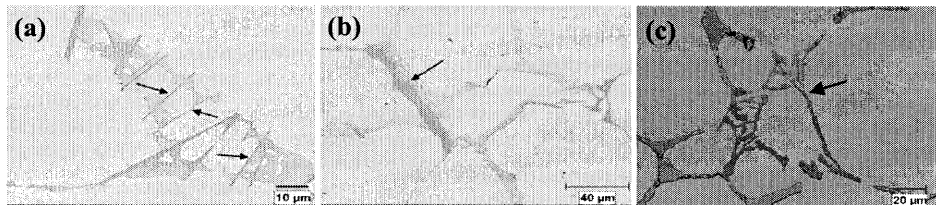


Figure 2 - Microstructures of various iron-containing intermetallics in Alloy 3  
(a) Eutectic β-Fe (Al<sub>7</sub>Cu<sub>2</sub>Fe), (b) Pre-eutectic β-Fe (Al<sub>7</sub>Cu<sub>2</sub>(FeMn)), (c) α-Fe (Al<sub>15</sub>(FeMn)<sub>3</sub>(SiCu)<sub>2</sub>)

To further disclose the morphologies of the iron-containing intermetallics, some selected specimens were deeply etched. Fig. 3 shows the typical three-dimensional morphologies of the iron-containing intermetallic phases. It can be seen that the eutectic  $\beta$ -Fe has a plate shape interwoven with the  $Al_2Cu$  phase in the Al matrix. In contrast, the pre-eutectic  $\beta$ -Fe in Fig. 3b is like a rod embedded in the Al matrix. As shown in Fig. 3c, the  $\alpha$ -Fe has a typical dendrite form. Many primary branches with different sizes grow from the center and some secondary branches can directly grow from the sides of the large primary branches.



Figure 3 - Three-dimensional morphologies of iron-containing intermetallics:  
 (a) Eutectic  $\beta$ -Fe, (b) Pre-eutectic  $\beta$ -Fe, (C)  $\alpha$ -Fe

**Effect of Mn and Si on Iron-containing Intermetallics**

The microstructures of Alloys 1-3 at 0.1 Si and various Mn contents are shown in Fig.4. It can be seen that almost all the iron-containing intermetallics in Alloy 1 with a Mn/Fe ratio of 0.3 are  $\beta$ -Fe (Fig. 4a). Even though many  $\beta$ -Fe particles are still present, the  $\alpha$ -Fe phase is observed in Alloy 2 with a Mn/Fe ratio of 0.67 (Fig. 4b). In Alloy 3 with a Mn/Fe ratio of 1.33, the amount of  $\beta$ -Fe is much less than that in Alloy 2 and  $\alpha$ -Fe has become the dominant Fe-rich phase. Hence, it can be concluded that the addition of Mn will be useful for the formation of  $\alpha$ -Fe. However, the presence of  $\beta$ -Fe phase at a high Mn/Fe ratio of 1.33 indicates that not all the  $\beta$ -Fe can transform to  $\alpha$ -Fe. Compared with Alloy 2, it can also be found that Alloy 6 (Fig. 6) has much less  $\beta$ -Fe and more  $\alpha$ -Fe, indicating that Si also has influence on the formation of iron-containing intermetallics in Al-Cu alloys. Further evidences of the effect of Si on the iron-containing intermetallics are shown in Fig. 5.

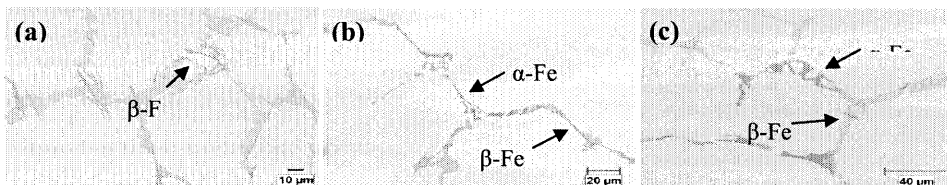


Figure 4 - Microstructures of iron-containing intermetallics in Alloys 1 - 3  
 (a) Alloy 1 (0.1Si+0.1Mn), (b) Alloy 2 (0.1Si+0.2Mn), and (c) Alloy 3 (0.1Si+0.4Mn)

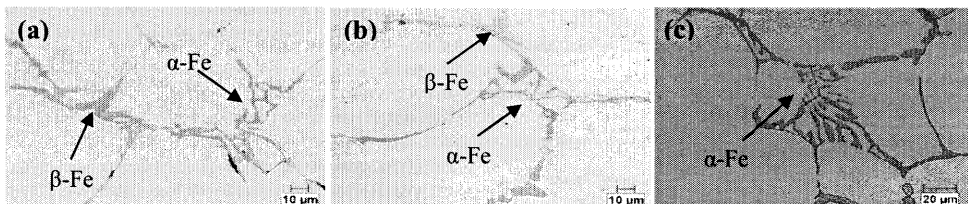


Figure 5 - Microstructures of iron-containing intermetallics in Alloys 4, 5 and 7  
 (a) Alloy 4 (0.2Si+0.1Mn) , (b) Alloy 5 (0.3Si+0.1Mn) , and (c) Alloy 7 (0.3Si+0.3Mn)

Compared with the microstructures shown in Fig.5, it can be found that Si has a similar effect with Mn on the transformation tendency of Fe-rich phases. The  $\alpha$ -Fe phase precipitates in Alloys 4 and 5 but there are still some  $\beta$ -Fe particles. In Alloy 7 with 0.3Si + 0.3Mn, however, almost all the Fe-rich particles are  $\alpha$ -Fe phase indicating the effective transformation of  $\beta$ -Fe into the  $\alpha$ -Fe phase. Additionally, compared with the results in Fig. 5b and Fig. 5c, it can be concluded that more addition of Mn with the same level of Si (0.3 wt. %) also favors the formation of the  $\alpha$ -Fe phase, which further confirms the role of Mn as an effective neutralization agent in Al-Cu alloys .

To quantify the iron-containing intermetallics, the relative volume fraction of the two iron-containing intermetallic phases has been measured using image analysis, as shown in Fig. 6. These quantified results are consistent with the general metallographic observations as discussed above. In general, the relative volume fraction of the  $\alpha$ -Fe phase increases when increasing the contents of Mn and/or Si. However, the individual addition of either Mn or Si cannot completely transform a  $\beta$ -Fe into a  $\alpha$ -Fe phase even at a high Mn/Fe level of 1.33 or a Si/Fe level of 1.0. At the 0.3 Si and 0.3 Mn levels in Alloy 7, the  $\beta$ -Fe has been effectively suppressed and hence almost all iron-containing intermetallics precipitate in the  $\alpha$ -Fe phase. This indicates that a combination of both high Si and Mn levels can completely transform  $\beta$ -Fe into a  $\alpha$ -Fe phase. Comparing Alloy 5 (0.3Si+0.1Mn) with Alloy 6 (0.2Si+0.2Mn), there is more  $\alpha$ -Fe precipitate in Alloy 6 indicating that Mn is a more effective element than Si to transform  $\beta$ -Fe into the  $\alpha$ -Fe phase. The results can also be further confirmed by the comparison of Alloy 2 (0.1Si+0.2Mn) and Alloy 4 (0.2Si+0.1Mn).

Fig. 7 shows the TA and DSC curves of Alloy 1. Compared with the curves in Fig. 1, it can be seen that there are only three peaks visible in Alloy 1 and these peaks correspond to the reactions shown in Table 2. It can clearly be seen that only  $\beta$ -Fe phase reactions (reactions 3 and 4) are present in Alloy 1 (0.1Mn+0.1Si). In contrast, the  $\alpha$ -Fe phase formed in Alloy 6 (0.2Si+0.2Mn), indicates that more addition of Mn and/or Si favors the formation of the  $\alpha$ -Fe phase. Furthermore, the peak intensity of pre-eutectic  $\beta$ -Fe (peak 3) is much weaker in Alloy 6 than in Alloy 1. Additionally, the formation temperature of the pre-eutectic  $\beta$ -Fe phase in Alloy 6 is also lower, about 580°C in Alloy 6 and 590°C in Alloy 1, indicating that the formation of the  $\beta$ -Fe phase has been effectively suppressed in Alloy 6. In summary, addition of Mn and/or Si favors the formation of the  $\alpha$ -Fe phase but suppresses the  $\beta$ -Fe phase and that Mn is a more effective neutralization agent than Si. The combined addition of both Mn and Si is even more effective than the individual addition of either Mn or Si.

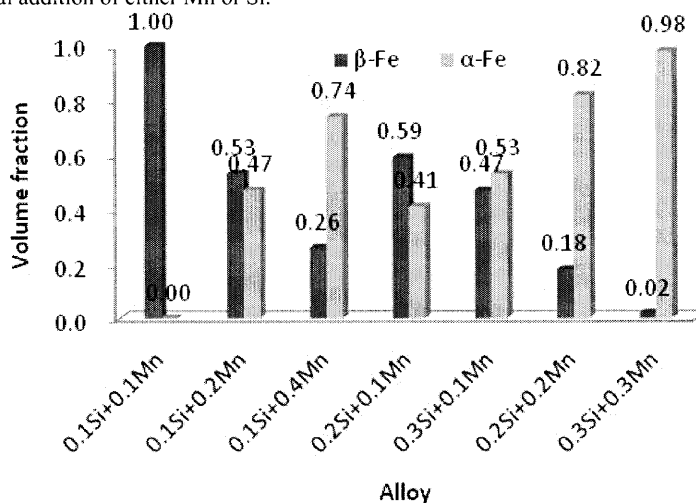


Figure 6 - Volume fraction of iron-containing intermetallics in Alloys 1 to 7

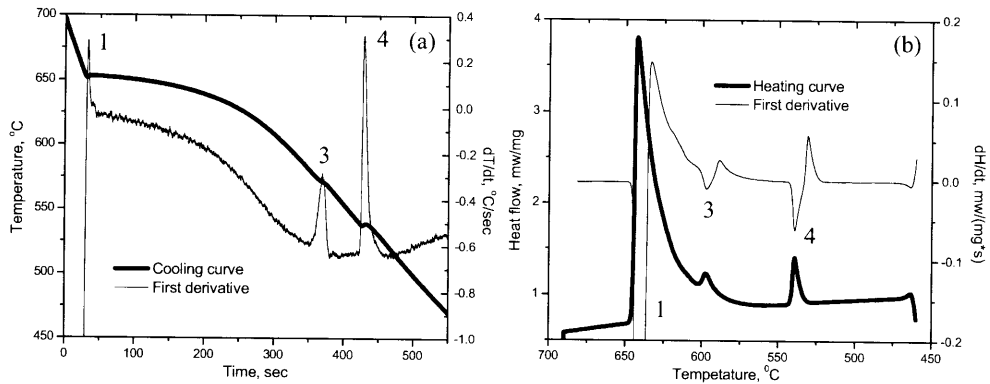


Figure 7 - TA and DSC curves of Alloys 1  
 (a) TA cooling curve and its first derivative, (b) DSC heating curve and its first derivative

## CONCLUSIONS

(1) There are mainly two types of iron-containing intermetallic phases in the final solidified structure of cast 206 aluminum alloy family: Chinese script  $\alpha$ -Fe ( $\text{Al}_{15}(\text{FeMn})_3(\text{SiCu})_2$ ), and platelet  $\beta$ -Fe ( $\text{Al}_7\text{Cu}_2\text{Fe}$  and  $\text{Al}_7\text{Cu}_2(\text{FeMn})$ ). The platelet  $\beta$ -Fe can precipitate in eutectic and/or pre-eutectic reactions. Due to a higher diffusion rate at a higher temperature, the pre-eutectic  $\beta$ -Fe platelets are longer and much thicker and hence have lower aspect ratios than the eutectic  $\beta$ -Fe phase.

(2) Either Si or Mn favors the transformation of  $\beta$ -Fe into the  $\alpha$ -Fe phase. Moreover, Mn is a more effective neutralization agent than Si. The individual addition of either Si or Mn cannot completely transform  $\beta$ -Fe into the  $\alpha$ -Fe phase even at a high Mn/Fe level of 1.33 or a Si/Fe level of 1.0.

(3) At a combination of both high Mn and high Si, almost all  $\beta$ -Fe platelets can be converted into Chinese script  $\alpha$ -Fe. For a cast Al-4.5Cu-0.3Fe alloy, 0.3% Mn and 0.3% Si are required to completely suppress the  $\beta$ -Fe phase.

## ACKNOWLEDGEMENTS

The authors would like to acknowledge the Natural Sciences and Engineering Research Council of Canada (NSERC) and Rio Tinto Alcan, through the NSERC-Rio Tinto Alcan Industrial Research Chair in Metallurgy of Aluminum Transformation at UQAC, for their financial support.

## REFERENCES

1. V.S. Zolotarevsky, N.A. Belov and M.V. Glazoff: Casting aluminum alloys, Elsevier, Oxford, UK, 2007.
2. L. Lu and A.K. Dahle, "Iron-rich intermetallic phases and their role in casting defect formation in hypoeutectic Al-Si alloy", Metall. Mater. Trans. A, Vol 36, 2005, 819-835.
3. A.M. Samuel, A. Pennorst, C. Villeneuve, F.H. Samuel, H.W. Doty and S. Valtierra, "Effect of cooling rate and Sr-modification on porosity and Fe-intermetallics formation in Al-6.5%Si-3.5% Cu-Fe alloys", Int. J. Cast Metals Res., Vol 13, 2000, 231-253.

4. S. Murali and K.S.S. Murthy, "Morphology studied on  $\beta$ -Al<sub>3</sub>FeSi phase Al-7Si-0.3Mg alloy with trace additions of Be, Mn, Cr and Co", *Material Characterization*, Vol 33, 1994, 99-112.
5. W. Khalifa, F.H. Samuel, J.E. Gruzleski, H.W. Doty and S. Valtierra, "Nucleation of Fe-intermetallic phases in the Al-Si-Fe alloys", *Metall. Mater. Trans. A*, Vol 36, 2005, 1017-1032.
6. J.Y. Hwang, H.W. Doty and M.J. Kaufman, "The effects of Mn additions on the microstructure and mechanical properties of Al-Si-Cu casting alloys", *Mater. Sci. Eng. A*, Vol 488, 2008, 496-504.
7. M.D. Cameron, A.T. John and K.D. Arne, "As-cast morphology of iron-intermetallics in Al-Si foundry alloys", *Scripta Materialia*, Vol 53, 2005, 955-958.
8. N. Roy, A. M. Samuel and F.H. Samuel, "Porosity formation in Al-9 Wt Pet Si-3 Wt Pet Cu alloy systems: Metallographic observations", *Metall. Mater. Trans. A*, Vol 27, 1996, 415-429.
9. P. Ashtari, H. Tezuka and T. Sato, "Influence of Sr and Mn additions on intermetallic compound morphologies in Al-Si-Cu-Fe cast alloys", *Materials Transactions*, Vol 44, 2003, 2611-2616.
10. X. Cao and J. Campbell, "The solidification characteristics of Fe-rich intermetallics in Al-11.5Si-0.4Mg cast alloys", *Metall. Mater. Trans. A*, Vol 35, 2004, 1425-1435.
11. The Aluminum Association: "Designations and Chemical Composition Limits for Aluminum Alloys in the Form of Castings and Ingot", Washington, D.C. USA , 2006.
12. L. Backerud, G. Chai, and J. Tamminen: *Solidification characteristics of aluminum alloys*, AFS/Akanaluminium, Stockholm, 1990.